COBEM 2021 26th International Congress of Mechanical Engineering
November 22-26, 2021, Virtual Congress, Brazil

COB-2021-0226
An experimental investigation on the fatigue behaviour of 304L stainless steel notched member subjected to axial-torsional loading

C. Bemfica
F. Castro
Department of Mechanical Engineering, University of Brasilia, 70910-900, Brasilia, DF, Brazil
cainabemfica@aluno.unb.br
fabiocastro@unb.br

Abstract. *This work investigates the axial-torsional fatigue and cyclic plasticity of notched 304L stainless steels specimens at room temperature. Fully reversed force- and torque-controlled axial, torsional and axial-torsional nonproportional loading paths were investigated, with fatigue lives ranging from 10^2 to 10^6 cycles. For selected specimens, rosette strain-gauges were placed at the notch root to investigate the local strains. The evolution of local strains is consistent with the cyclic hardening behaviour observed in thin-walled tubular specimens. An initial cyclic softening is observed and may be followed by secondary hardening due to martensitic transformation. Measurable plastic strains were observed for all tests, including those that did not fail after 10^6 cycles. A post-mortem analysis of the fracture surface indicates that multiple crack initiation sites were observed for axial, torsional and nonproportional loading for low fatigue lives ($<10^5$ cycles). Moreover, the failure mechanism under torsional loading depends on the fatigue life regime: for lower fatigue lives, fatigue cracks exhibited orientations that correspond to the plane of maximum normal stress, whilst orientations corresponding to the plane of maximum shear stress were observed for longer fatigue lives ($>10^5$ cycles).*

Keywords: *stainless steel, notched specimens, multiaxial fatigue, cyclic plasticity*

1. Introduction

Fatigue life prediction depends on how accurately stress and/or strain can be obtained. For geometries like thin-walled tubular specimens, stress states can be reasonably estimated from force and torque measures, thus being a useful geometry to develop both fatigue criteria and cyclic plasticity models. One limitation of thin-walled tubular specimens is that stress and strain states found in engineering components, such as gradient effects due to notches, may not be reproduced by using these specimens. Hence, an evaluation of fatigue criteria and cyclic plasticity models for stress and strain states not covered by thin-walled tubular specimens can be useful to engineering design. Notched specimens can be one useful alternative, since multiaxial stress and strain states may arise at the vicinity of the notch root even for uniaxial loading. Moreover, since many engineering components have notches, this geometry may produce more suitable data to engineering design than those obtained from thin-walled tubular specimens.

The axial-torsional fatigue of stainless steel notched specimens has been the subject of few previous investigations. Sakane and Ohnami (1986) investigated the uniaxial low-cycle fatigue of 304 stainless steel with three different round notch geometries at 600 °C, whilst Bayoumi and Abd El Latif (1995) investigated semi-circle and V-notches at room temperature. Under torsional loading, Ohkawa and Ohkawa (2011) and Tanaka (2014) investigated fatigue behaviour of 316NG and 316L stainless steel, respectively. The authors observed a notch-strengthening effect, with longer lives being observed for sharper notches under the same nominal shear stress. This effect was related to the serrated factory-roof type crack faces, which delayed the crack growth, thus extending fatigue life. Note that the works of Ohkawa and Ohkawa (2011) and Tanaka (2014) addressed a fatigue life regime greater than 10^5 cycles. For this fatigue life regime, macroscopic fatigue crack orientation may be compatible with the plane of maximum tensile stress under torsional loading (Sakane and Itoh, 2018), which is not observed for lives less than 10^5 cycles (Bemfica *et al.*, 2019). Under nonproportional loading, Morishita and Itoh (2016) investigated the axial-torsional fatigue behaviour of 316L stainless steel, addressing the influence of the notch geometry for a single equivalent strain amplitude. Based on the aforementioned investigations, one should observe that a comprehensive evaluation of the fatigue behaviour and cyclic plasticity of stainless steel notched specimens, regarding both loading paths and amplitudes, must be carried out.

In this work, the fatigue and cyclic stress-strain behaviour of 304 stainless steel notched specimens are investigated at room temperature. Three fully reversed force and/or torque-controlled loading paths were investigated: tension-compression, torsional and 90° out-of-phase. The loading amplitudes used in the tests resulted in fatigue lives ranging from 10^3 to 10^6 cycles. After failure, the fracture surface will be analysed to determine the locus of fatigue crack initiation and the fatigue cracking behaviour.

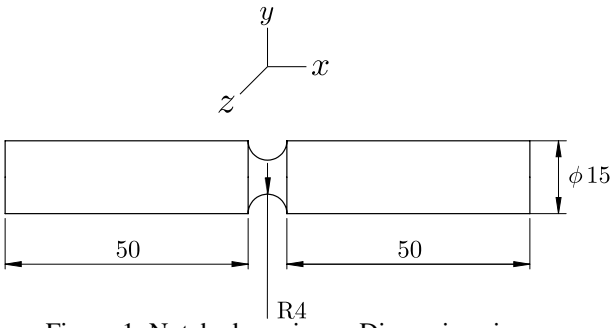

Figure 1: Notched specimen. Dimensions in mm.

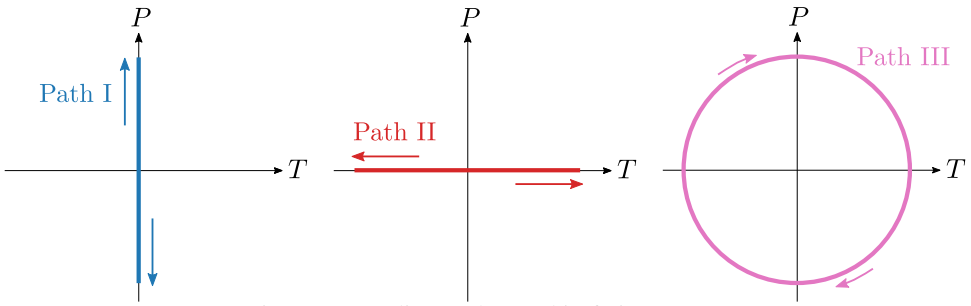

Figure 2: Loading paths used in fatigue tests.

2. Experimental programme and test data

The 304L stainless steel was received as extruded bars with a diameter of 19.05 mm. The chemical composition and monotonic properties of this material can be found in a previous publication (Bemfica *et al.*, 2019). Circumferentially notched specimens with the geometry and dimensions as shown in Fig. 1 were machined from the extruded bars. The elastic stress concentration factors of the notched specimen were K_{tc} = 1.43 for tension-compression and K_{tor} = 1.14 for torsional loading (Peterson, 1974). This geometry was selected because it gives the largest stress concentration factor while providing access to the notch root for the strain gauge installation. After machining, specimens were normalized at 1050 °C for 1 h to diminish the residual stresses related to both the extrusion and the machining processes. Afterwards, the outer surface of the notched section was ground using sandpapers with 220 up to 2500 grit to minimize the effects of surface finishing.

All tests were performed at room temperature using an MTS 809 axial-torsional servo-hydraulic machine, which is equipped with a load cell of capacity ±100 kN for axial force and ±1100 N·m for torque. For selected tests, miniature rosette strain gauges with a gauge length of approximately 0.8 mm were used to measure notch root strains. Local strains could not be measured from the beginning to the end of all tests due to strain gauge failure. To ensure that the strain gauge was properly installed, strain measures at the notch root of a dummy specimen were compared with those simulated by elastic finite element analysis (FEA). The difference between the amplitude obtained from the strain gauge and the one obtained from FEA simulation was approximately 7.5%.

Three fully reversed force and torque-controlled axial-torsional loading paths were investigated and are illustrated in Fig. 2, where P and T are the applied axial force and torque, respectively: tension-compression (Path I), torsional (Path II) and 90° out-of-phase nonproportional (Path III). Tests were conducted until complete failure or run-out (10^6 cycles). For all tests, the evolutions of displacement and twist angle were monitored to distinguish between the microscopic (initiation and early propagation) and macroscopic (visible to the naked eye) crack growth. In this sense, the initiation and early propagation phases can be understood as the phases in which the macroscopic stress-strain behaviour is not influenced by the presence of the fatigue crack. This interpretation is consistent with fatigue analyses based on macroscopic stress-strain measures, which usually cannot take into account the complex phenomena involved into the initiation and early propagation phases (Sangid, 2013). For all tests, the macroscopic crack growth phase was not significant when compared to the total life, as also observed by Gao *et al.* (2010) for force- and torque-controlled tests. After failure, the locus of fatigue crack initiation was determined based on the morphology of the fracture surface analysed using a JEOL JSM-7100F Scanning Electron Microscope (SEM).

The loading frequencies of fatigue tests were chosen considering the rate-dependent stress-strain behaviour of the 304L stainless steel (Krempl and Lu, 1984; Kang *et al.*, 2006). For all loading paths, strains at the notch root of a dummy specimen were monitored for a selected range of loading frequencies and amplitudes. Test frequencies were those that produced an equivalent strain rate $\dot{\varepsilon}_{\mathrm{eq}} = \sqrt{2/3}||\dot{\boldsymbol{\varepsilon}}||$ whose order of magnitude was equal to $10^{-2}\ s^{-1}$ for all loading conditions. Note that this equivalent strain range is within the strain rate adopted in a previous investigation for solid and

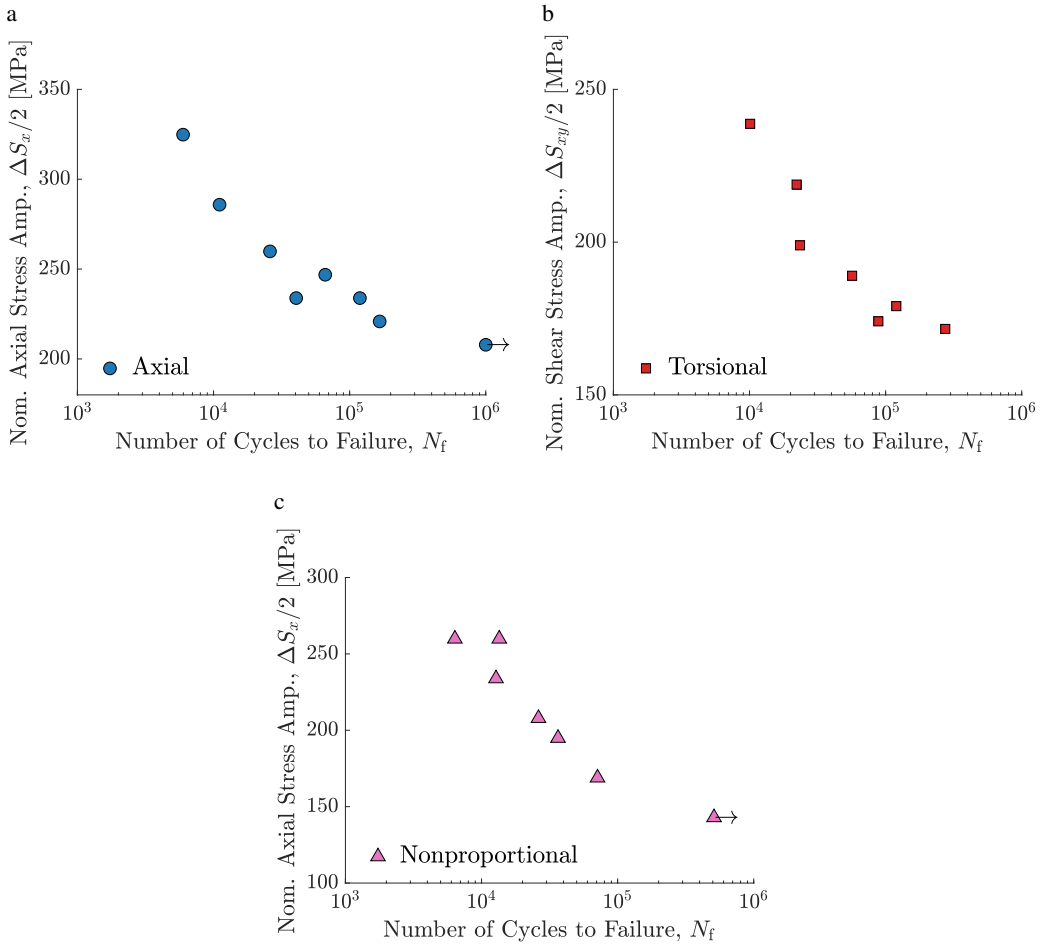

Figure 3: Fatigue test results for a) tension-compression, b) torsional, and c) 90° nonproportional loading.

thin-walled tubular specimens (Bemfica *et al.*, 2019). This procedure intends to minimize the influence of the loading rate on the fatigue and on the cyclic stress-strain behaviour of 304L stainless steel. Hence, a rate-independent analysis can be carried out, notwithstanding the rate-dependent behaviour of this material.

A summary of fatigue test data is presented in Table 1. Nominal stresses were calculated based on the net section. Note that these nominal values may not reflect actual stresses, thus an equivalent measure based on nominal stresses to compare different loading paths would have no physical meaning. Hence, test data shown in Fig. 3 are not combined in a single plot since they cannot be directly compared. In Fig. 3, run-out tests are denoted by an arrow.

3. Results and discussion

3.1 Strain measurement at notch root

The cyclic softening/hardening of the 304L stainless steel can be investigated based on the evolution of strain measures obtained at the notch root from the rosette strain gauges. Due to premature failure of strain gauges, the evolution of local strains could not be investigated for all tests and, therefore, only strain measures prior to strain gauge failure—represented by an X in Fig. 4—are considered. Note that the strain gauge did not fail only for the run-out axial test ($\Delta P = 8.0$ kN), thus being a useful test to investigate the late cyclic stress-strain behaviour. The evolution of notch strains is shown in Fig. 4 for selected axial tests. During the initial cycles, an increase on axial, hoop and shear strain components is observed, suggesting an initial cyclic softening also observed for solid and thin-walled tubular specimens (Bemfica *et al.*, 2019). For the run-out axial test, a second stage was observed, with both strain components diminishing after achieving its maximum value around 10^5 cycles, suggesting a secondary hardening. This behaviour is similar to the one observed for solid and thin-walled specimens and is probably related to a plastic strain-induced martensitic transformation (Bemfica *et al.*, 2019). Note that the plastic strain-induced transformation can occur without any temperature change, unlike the martensitic transformation observed after rapid cooling (Bayerlein *et al.*, 1989). For the remaining experiments, it cannot be known whether that martensitic transformation occurred based on the local strain measures.

For solid and thin-walled tubular specimens, measurable plastic strains were observed even for tests that did not fail

Table 1: Fatigue test data for the notched 304L stainless steel.

Loading Path	Specimen	$\Delta P/2$ [kN]	$\Delta S_x/2$ [MPa]	$\Delta T/2$ [N·m]	$\Delta S_{xy}/2$ [MPa]	f [Hz]	N_f [Cycles]
Axial	NO08	12.5	324.8	–	–	0.50	5,973
	NO07	11.0	285.8	–	–	0.75	11,071
	NO02	10.0	259.8	–	–	1.00	25,987
	NO05	9.5	246.9	–	–	1.30	66,154
	NO06	9.0	233.9	–	–	1.50	40,479
	NO17	9.0	233.9	–	–	1.50	118,920
	NO19	8.5	220.9	–	–	1.75	166,165
	NO04	8.0	207.9	–	–	2.50	>1,000,000
Torsional	NO13	–	–	24.0	238.7	0.20	10,110
	NO10	–	–	22.0	218.8	0.30	22,173
	NO09	–	–	20.0	198.9	0.40	23,499
	NO12	–	–	19.0	189.0	0.50	56,732
	NO11	–	–	18.0	179.0	0.70	119,870
	NO14	–	–	17.5	174.1	0.90	88,442
	NO16	–	–	17.5	174.1	0.90	274,299
Nonproportional	NO27	10.0	259.8	17.3	172.3	0.30	6,371
	NO25	10.0	259.8	17.3	172.3	0.30	13,494
	NO22	9.0	233.9	15.6	155.1	0.40	12,776
	NO18	8.0	207.9	13.9	137.8	0.60	26,208
	NO21	7.5	194.9	13.0	129.2	0.70	36,476
	NO24	6.5	168.9	11.3	112.0	0.90	71,152
	NO26	5.5	142.9	9.5	94.8	1.30	>510,715

$\Delta P/2$, Axial force amplitude; $\Delta S_x/2$, Nominal axial stress amplitude; $\Delta T/2$, Torque amplitude; $\Delta S_{xy}/2$, Nominal shear stress amplitude; f, Frequency; N_f, Number of cycles to failure.

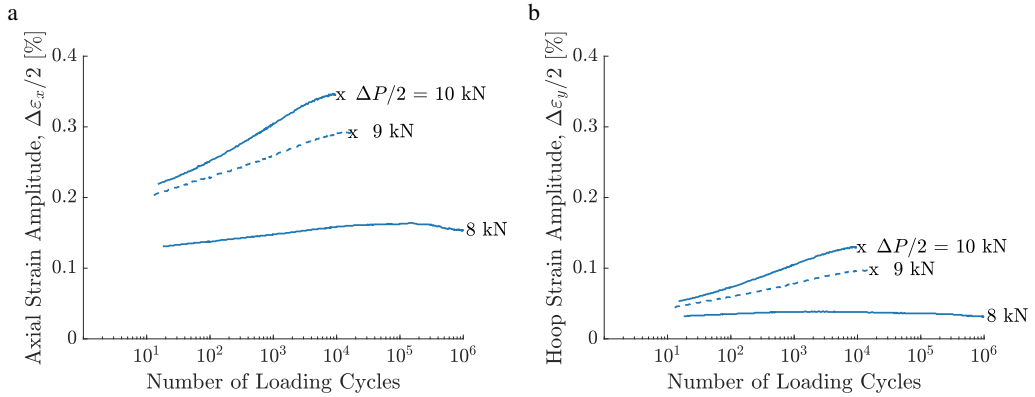

Figure 4: Evolution of a) axial and b) hoop strains at the notch root for selected axial tests. Shear strains are less than 0.05% and are not shown. The symbol X denotes strain gauge failure.

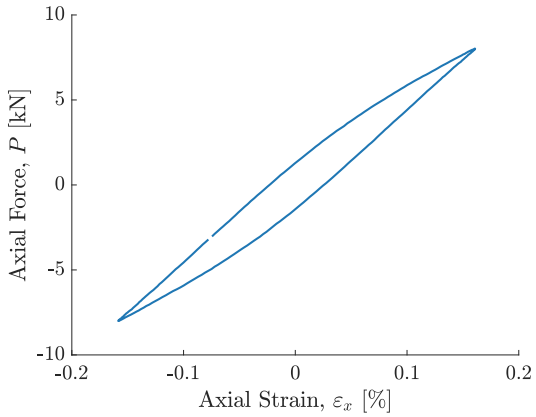

Figure 5: Plot of axial force vs. axial strain for run-out test ($\Delta P/2 = 8.0$ kN) at maximum softening.

after 10^6 cycles. This trend was also observed for notched specimens, as shown in Fig. 5 for the run-out test in the plot axial force vs. axial strain. Note that plastic strain amplitude was around 0.05%, approximately 30% of the total strain amplitude. This result shows the importance of considering the cyclic plasticity behaviour of 304L stainless steel even for a fatigue life regime usually associated with little or no macroscopic plastic strains.

3.2 Cracking behaviour

To investigate the fatigue cracking behaviour, a *post-mortem* analysis of the fracture surface was carried out at a scanning electron microscope. For each loading path, two characteristic surfaces are shown in Fig. 6. For axial loading (Fig. 6a and 6b), initiation sites are located in the plane of maximum tensile stress. For lower fatigue lives (Fig. 6a), the presence of dimples (delimited region, shown in Fig. 7 for specimen NO25) at the centre of the surface suggests that multiple initiation sites occurred, which did not occur for greater fatigue lives (Fig. 6b). For torsional loading (Fig. 6c and 6d), two very distinct morphologies were observed: for lower fatigue lives, initiation sites are located in the plane of maximum shear stress, whilst a factory-roof morphology compatible with the planes of maximum tensile stress for greater fatigue lives. Note that factory-roof surfaces are also observed by Tanaka (2014) for the 316 stainless steel for the same fatigue life range (around 10^5 cycles). For nonproportional loading, a trend similar to axial loading was observed regarding multiple initiations, with no significant difference between fracture surface orientations being observed for the investigated fatigue life regime.

The fatigue cracking behaviour dependence on the fatigue life regime under torsional loading was also observed for thin-walled specimens (Bemfica *et al.*, 2019; Sakane and Itoh, 2018). Moreover, the fatigue life regime at which the cracking behaviour varies is compatible with the regime observed for thin-walled specimens, around 10^5 cycles. One possible explanation is the similarity between the stress states of both specimens under torsional loading since a pure shear stress state is observed at the notch root for both specimens.

4. Conclusions

The fatigue and cyclic plasticity of 304L stainless steel notched specimens were investigated at room temperature. Tests were performed under fully reversed force- and/or torque-controlled loading. The loading conditions used were: axial, torsion, and 90° out-of-phase (nonproportional). For selected tests, notch strains were measured using a rosette strain gauge. The main observations and conclusions can be summarized as follows:

1. Due to the relatively short life of the strain gauges, it was not possible to record for all tests the notch strain evolution until test termination. Nevertheless, it was possible to observed an initial cyclic softening for all axial tests. For the only axial test during which the strain gauge did not prematurely fail, secondary hardening was observed.

2. Measurable macroscopic plastic strains were observed at the notch root of all axial tests, including the run-out tests. Inconclusive measures were obtained for the torsional tests due to strain gauge failure.

3. The fatigue cracking behaviour of notched specimens was similar to the one observed for solid and thin-walled tubular specimens. For torsional loading, a transition from shear to tensile mode was observed around 10^5 cycles.

5. Acknowledgements

This study was financed in part by the Coordenação de Aperfeiçoamento de Pessoal de Nível Superior - Brasil (CAPES) - Finance Code 001. Fábio Castro would like to acknowledge the support from the National Council for Scien-

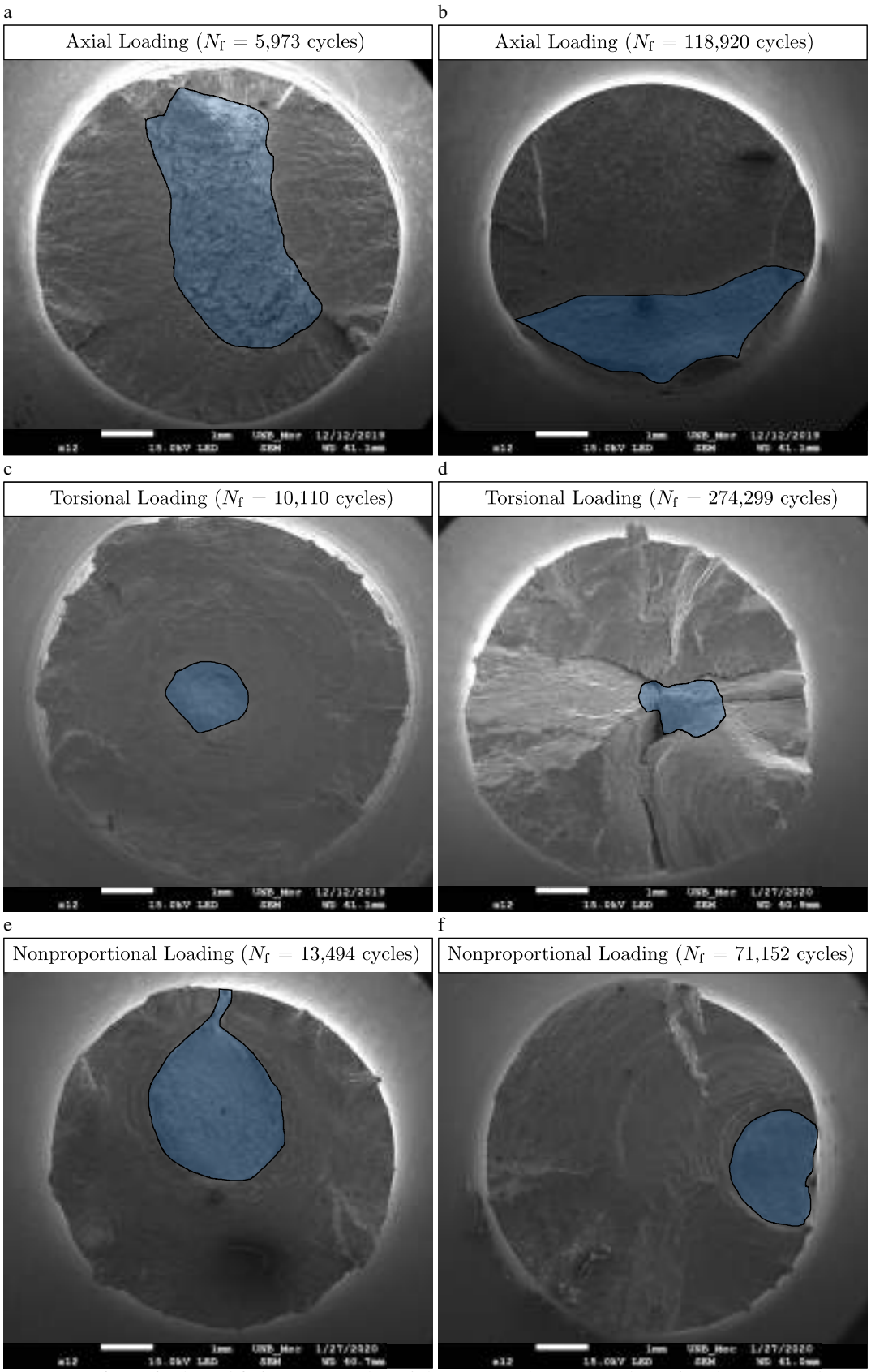

Figure 6: Fracture surface of selected fatigue tests: a,b) axial (NO08 and NO17); c,d) torsional (NO13 and NO16) and e,f) nonproportional (NO25 and NO24) loading. The delimited area are the regions where dimples were observed.

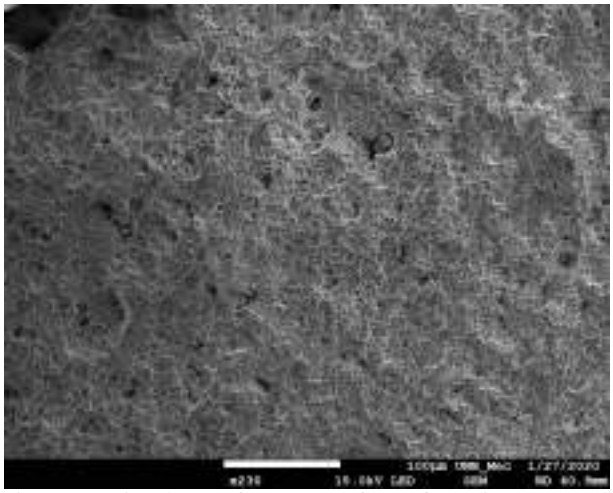

Figure 7: Dimples on fracture surface of specimen NO25.

tific and Technological Development – CNPq (contracts 307330/2019-2 and 420677/2018-6).

6. References

Bayerlein, M., Christ, H.J. and Mughrabi, H., 1989. "Plasticity-induced martensitic transformation during cyclic deformation of AISI 304L stainless steel". *Materials Science and Engineering A*, Vol. 114, No. C, pp. L11–L16. ISSN 09215093. doi:10.1016/0921-5093(89)90871-X.

Bayoumi, M.R. and Abd El Latif, A.K., 1995. "Low-cycle fatigue behaviour of notched AISI 304 stainless steel specimens". *Journal of Materials Science*, Vol. 30, No. 15, pp. 3944–3953. ISSN 00222461. doi:10.1007/BF01153961.

Bemfica, C., Carneiro, L., Mamiya, E.N. and Castro, F.C., 2019. "Fatigue and cyclic plasticity of 304L stainless steel under axial-torsional loading at room temperature". *International Journal of Fatigue*, Vol. 125, pp. 349–361. ISSN 01421123. doi:10.1016/j.ijfatigue.2019.04.009.

Gao, Z., Qiu, B., Wang, X. and Jiang, Y., 2010. "An investigation of fatigue of a notched member". *International Journal of Fatigue*, Vol. 32, No. 12, pp. 1960–1969. ISSN 0142-1123. doi:10.1016/j.ijfatigue.2010.07.005.

Kang, G., Kan, Q., Zhang, J. and Sun, Y., 2006. "Time-dependent ratchetting experiments of SS304 stainless steel". *International Journal of Plasticity*, Vol. 22, No. 5, pp. 858–894. ISSN 07496419. doi:10.1016/j.ijplas.2005.05.006.

Krempl, E. and Lu, H., 1984. "Hardening and Rate-Dependent Behavior of Fully Annealed Aisi Type 304 Stainless Steel Under Biaxial in-Phase and Out-of-Phase Strain Cycling At Room Temperature". *Journal of Engineering Materials and Technology, Transactions of the ASME*, Vol. 106, No. 4, pp. 376–382. ISSN 00944289. doi:10.1115/1.3225733.

Morishita, T. and Itoh, T., 2016. "Evaluation of multiaxial low cycle fatigue life for type 316L stainless steel notched specimen under non-proportional loading". *Theoretical and Applied Fracture Mechanics*, Vol. 84, pp. 98–105. ISSN 01678442. doi:10.1016/j.tafmec.2016.02.007.

Ohkawa, C. and Ohkawa, I., 2011. "Notch effect on torsional fatigue of austenitic stainless steel: Comparison with low carbon steel". *Engineering Fracture Mechanics*, Vol. 78, No. 8, pp. 1577–1589. ISSN 00137944. doi: 10.1016/j.engfracmech.2011.01.015.

Peterson, R.E., 1974. *Stress Concentration Factors*. ISBN 9781119532521. doi:10.1115/1.3423544.

Sakane, M. and Itoh, T., 2018. "A synthesis of cracking directions in tension-torsion multiaxial low cycle fatigue at high and room temperatures". *Theoretical and Applied Fracture Mechanics*, Vol. 98, No. January, pp. 13–22. ISSN 01678442. doi:10.1016/j.tafmec.2018.09.003.

Sakane, M. and Ohnami, M., 1986. "Notch effect in low-cycle fatigue at elevated temperatures-life prediction from crack initiation and propagation considerations". *Journal of Engineering Materials and Technology, Transactions of the ASME*, Vol. 108, No. 4, pp. 279–284. ISSN 15288889. doi:10.1115/1.3225883.

Sangid, M.D., 2013. "The physics of fatigue crack initiation". *International Journal of Fatigue*, Vol. 57, pp. 58–72.

Tanaka, K., 2014. "Crack initiation and propagation in torsional fatigue of circumferentially notched steel bars". *International Journal of Fatigue*, Vol. 58, pp. 114–125. ISSN 01421123. doi:10.1016/j.ijfatigue.2013.01.002.

7. Responsibility Notice

The authors are solely responsible for the printed material included in this paper.